# Solution-phase template approach for the synthesis of $Cu_2S$ nanoribbons

**Zhengquan Li,[a,b] Huan Yang,[b] Yue Ding,[b] Yujie Xiong†[b] and Yi Xie*[a,b]**

***Received 30th August 2005, Accepted 26th October 2005***
***First published as an Advance Article on the web 10th November 2005***
**DOI: 10.1039/b512205h**

In this paper, we have developed a solution-phase template approach to synthesize $Cu_2S$ nanoribbons for the first time. $Bi_2S_3$ nanoribbons act as both template and reactant when treated with small CuCl particles, generating $Cu_2S$ nanoribbons with the assistance of the solvent ethanol. Nanoribbons with different compositions of $Bi_2S_3$ and $Cu_2S$ also could be obtained through controlling the reaction time. This kind of template method is expected to be a general template approach due to its slow reaction rate and simplicity.

## Introduction

In recent years, one-dimentional (1D) nanostructures such as nanorods, nanowires and nanotubes have been shown to exhibit superior electrical, optical, mechanical and thermal properties, and are expected to be used as fundamental building blocks for nano-scale science and technology.[1,2] As a notable kind of 1D nanostructure with special geometrical shapes, nanoribbons (or nanobelts) have a rectangular cross section with a high surface-to-volume ratio, and thus show many potential applications in the field effect transistors and gas sensors *etc.*[3,4] Previous research has promoted several approaches for the synthesis of nanoribbons, such as the vapor–liquid–solid process, hydrothermal synthesis, *etc*., in which a variety of nanoribbons have been successfully obtained.[5–8] In general, the growth in the above cases was directed by the anistropic crystal structures under specific conditions. But, as it is hard to find a template as scaffold within which the as-desired materials can be generated *in situ* and shaped into ribbons, the template approach has seldom been used to fabricate nanoribbons. Therefore, the development of effective template approaches toward nanoribbons is of great significance.

Transition-metal chalcogenide nanocrystals have been extensively investigated for their potential applications to catalyst, solar cell, photoluminescence and optical devices.[9,10] As a type of indirect bandgap semiconductor, $Cu_2S$ nanocrystals are expected to be a distinguished candidate for optical devices.[11] In the past few years, several kinds of $Cu_2S$ nanocrystals, including nanorods and nanowires, have been synthesized. As examples, $Cu_2S$ nanorods, nanodisks and nanoplates were prepared *via* pyrolysis of precursors.[12,13] Well-arranged $Cu_2S$ nanorods were also obtained through a gas–solid reaction on copper foil, and their field emission properties were also investigated.[14,15] However, the synthesis of $Cu_2S$ nanoribbons still remains largely unexplored up to now.

[a]*School of Chemical and Material Engineering, Southern Yangtze University, Wuxi, Jiangsu, 214036, P. R. China. E-mail: yxielab@ustc.edu.cn; Fax: +86-551-3603987; Tel: +86-551-3603987*

[b]*Nano-materials and Nano-chemistry, Hefei National Laboratory for Physical Sciences at Microscale, University of Science and Technology of China, Hefei, Anhui, 230026, P. R. China*

† Present address: Department of Chemistry, University of Washington, Seattle, WA, 98195-1700, USA.

It is known that solid-state reactions generally proceed at a slow rate that facilitates control over chemical composition, but has the shortcoming that it generally produces solid-state by-products. Following the idea that by-products can be rationally removed by solvent in reaction processes, solid-state powders with specific nanostructures can be used as reactants as well as templates in the solution-phase. In this paper, we report the design of a novel solution-phase template approach to synthesize $Cu_2S$ nanoribbons. This new strategy could be illustrated as follows:

$$Bi_2S_3 + 6CuCl \rightleftarrows 3Cu_2S \downarrow + 2BiCl_3$$

In this reaction, solid-state $Bi_2S_3$ nanoribbons were used as both template and reactant that reacted with solid-state CuCl thin particles with the assistance of the solvent ethanol, as the by-product $BiCl_3$ could be completely dissolved in ethanol. As a result, ultra-long $Cu_2S$ nanoribbons were synthesized with a similar morphology to the reactant $Bi_2S_3$ nanoribbons. To the best of our knowledge, this is the first synthesis of $Cu_2S$ nanoribbons. This kind of template method is expected to be a general template approach due to its slow reaction rate and simplicity.

## Experimental

The reactant $Bi_2S_3$ nanoribbons were synthesized according to the literature.[16] Then the $Bi_2S_3$ nanoribbons (0.5138 g, 1 mmol) and excess ground CuCl powder (1.5905, 10 ml) were mixed and loaded in a 60 mL Teflon-lined autoclave which was filled with 50 mL absolute ethanol. The autoclave was sealed and maintained at 120 °C for 2 days, and then cooled to room temperature naturally. The precipitate was filtered off, washed with dilute HCl, distilled water, ammonia and absolute ethanol (to remove the by-products) several times, respectively, and dried under vacuum. The yield of $Cu_2S$ nanoribbons was approximately 82% referred to reactant $Bi_2S_3$.

## Results and discussion

The X-ray powder diffraction (XRD) analysis was performed on a Phillps X'pert PRO SUPPER diffractor equipped with Ni-flitered Cu-K$\alpha$ radiation ($\lambda = 1.54178$ Å). The XRD patterns of prepared products are shown in Fig. 1. All the peaks in Fig. 1 could be clearly indexed to the pure cubic phase of $Cu_2S$ (JCPDS 84–1770)

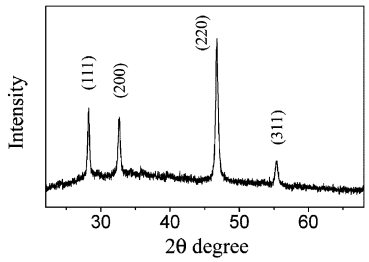


**Fig. 1** XRD patterns of prepared $Cu_2S$ nanoribbons.

with lattice constants $a = 5.628$ Å. No peaks for other types of $Cu_2S$ or impurities were observed in the XRD patterns, indicating high purity and crystallinity of the products.

The morphologies of the products were investigated by the field emission scanning electron microscope (FESEM, JEOL-6300). A typical FESEM image of the products is shown in Fig. 2A, revealing that the products consist of long wire-like structures. From the magnified FESEM image shown in Fig. 2B, one can clearly see that the thickness of the wire-like structures is different from their width, indicating that the products were of $Cu_2S$ nanoribbons rather than nanowires. Observation of a single nanoribbon is shown in Fig. 2C, showing the characteristic morphology of the ribbon-like structure. The thickness and width of these nanoribbons are about 20–80 nm and 50–300 nm, respectively, while their length usually reaches several millimeters long. The products were further studied by transmission electron microscopy (TEM, H-800) and high-resolution transmission electron microscopy (HRTEM, JEOL-2010). The TEM images in Fig. 2D and 2E also show the characteristics of ribbon-like morphologies, consistent with the FESEM observations. The inset of Fig. 2E shows the electron diffraction (ED) pattern of a single nanoribbon, which shows that the nanoribbon is a single crystal. The HRTEM image in Fig. 2F also shows the good crystallinity of the nanoribbons. The fringes (inset of Fig. 2F) are separated by about 2.0 Å, which agrees with the (220) lattice spacing of the $Cu_2S$ crystal. Note that the as-prepared $Cu_2S$ nanoribbons have inherited the length, width and thickness of those of the reactant $Bi_2S_3$ nanoribbons, suggesting that the $Bi_2S_3$ nanoribbons have acted as effective templates in the reaction process.

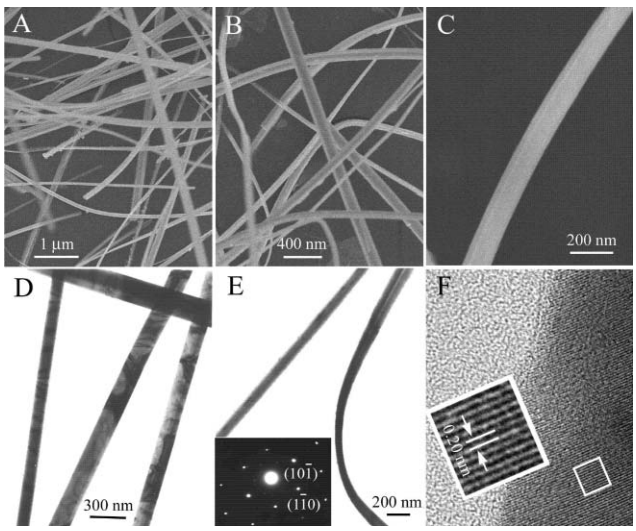


**Fig. 2** (A), (B) and (C) are FESEM images of $Cu_2S$ nanoribbons with different magnifications; (D) and (E) are the TEM images of $Cu_2S$ nanoribbons. The inset of E is the ED pattern of a single ribbon; (F) is a typical HRTEM image of $Cu_2S$ nanoribbons.

In the whole reaction process, only the by-product $BiCl_3$ could be dissolved in ethanol, which reduced the Gibbs Energy of this reaction and ensured the completeness of the solid–solid reaction. If water was used as solvent, this reaction could not happen because all the reactants and products could not be dissolved in it. On the other hand, when $Cu^+$ solution was used instead of CuCl particles, no $Cu_2S$ was produced either, indicating that a solid–liquid reaction between solid $Bi_2S_3$ and $Cu^+$ in solution did not happen under the same conditions. The above results suggest that the reaction between $Bi_2S_3$ and CuCl was a solid–solid one, which could increase the reaction entropy more than a solid–liquid or liquid–liquid interaction.

In order to investigate the possible formation mechanism of the $Cu_2S$ nanoribbons, we took samples at different reaction stages. The products at $t = 8$ h, 16 h and 24 h were collected, whose morphologies were also investigated by FESEM. The FESEM results indicated that no distinct morphologies were found in these intermediate products. A typical morphology of the intermediate product obtained at $t = 16$ h was shown in Fig. 3. From the panoramic image (Fig. 3A), one could see that the intermediates were composed of nanoribbons and irregular particles. Careful observation of the nanoribbon shown in Fig. 3B (and the inset) reveals that the surface of the nanoribbons are also covered by many thin nanoparticles. This indicates that the the small CuCl particles could easily transfer to the surface of $Bi_2S_3$ nanoribbons and react with them under the solvent–thermal conditions, while the large particles showed less activity. Note that the CuCl particles had a broad size distribution in the intermediate, resulting from the grinding pre-treatment. In our experiments, thanks to the inactivity of large CuCl particles, the added CuCl should be more than three times the stoichiometric amount for the production of pure $Cu_2S$ after completion of the reaction. The excess CuCl particles could be completely removed by diluted HCl.

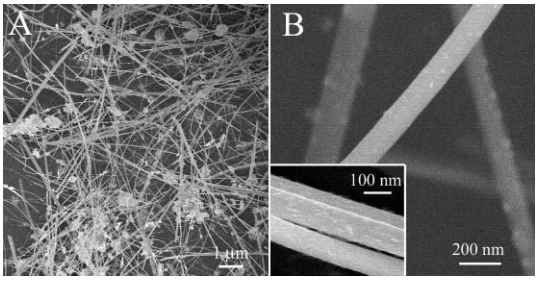


**Fig. 3** Morphologies of intermediate products prepared for 16 h. (A) Panoramic image; (B) magnified image. The inset is the magnified image of the surface of the nanoribbons.

Generally, the slow reaction rate facilitates control over the chemical composition of the products. In the present case, the solvent-assisted reaction was also found to be a slow one, though it was carried out at 120 °C. The XRD patterns of the intermediate products obtained at $t = 8$ h, 16 h and 24 h, after the by-products were washed leaving pure sulfide behind, are shown in Fig. 4A, 4B and 4C, respectively. From the patterns, one can see that there is

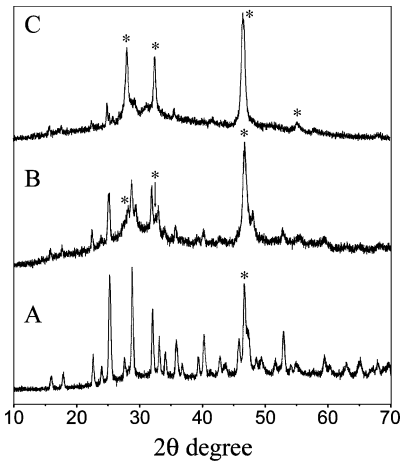


**Fig. 4** XRD patterns of the intermediate products prepared over different reaction times. (A) 8 h; (B) 16 h; (C) 24 h. The peaks marked with * belong to $Cu_2S$ while the others belong to $Bi_2S_3$. Note that $Bi_2S_3$ has complicated peaks.

an obvious shift from $Bi_2S_3$ (JCPDS 17–320) to $Cu_2S$ (JCPDS 84–1770) upon reaction. The elemental analyses of these intermediate products also determined that the content of Bi decreased along with the reaction time while that of Cu increased. These results show that the chemical compositions of the nanoribbons can be rationally controlled *via* the solution-phase template approach. Definitely, we obtained $Cu_2S/Bi_2S_3$ nanoribbons with different compositions in these intermediate products.

The intermediate products composed of $Cu_2S/Bi_2S_3$ nanoribbons were also investigated by HRTEM. Typical HRTEM images of the products obtained at $t = 8$ h are shown in Fig. 5. From the HRTEM image with low magnification (Fig. 5A), one can clearly see that the surface of the nanoribbons is very uneven, revealing that the reaction did not synchronously happen at the surface of the $Bi_2S_3$ nanoribbons. Closer inspection of the nanoribbons at different regions (Fig. 5A and 5B) shows that

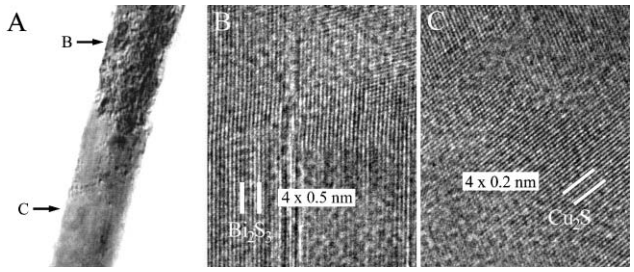


**Fig. 5** HRTEM images of the intermediate product obtained at $t = 8$ h. (A) Typical image of a single nanoribbon; (B) magnified image showing the dominant fringes of $Bi_2S_3$; (C) magnified image showing the dominant fringes of $Cu_2S$. Note that four fringes contained between the two white bars.

many faults and mismatches have appeared. However, note that the dominant fringes at different regions can be indexed to different compounds. For example, the marked places could be indexed to the (−210) lattice spacing of $Bi_2S_3$ and the (220) lattice spacing of $Cu_2S$, respectively. The HRTEM observation of the products obtained at $t = 16$ h and 24 h also showed similar results. The above results show that the reaction of $Bi_2S_3$ and CuCl does not happen synchronously at all regions, which confirmed the FESEM observation that the thin CuCl particles did not cover the surface of $Bi_2S_3$ uniformly. Note that whether the reaction between $Bi_2S_3$ and CuCl in ethanol definitely belongs to a solid–solid one is not very clear, although the studies of the intermediates suggest that it is. Further investigation of the detailed reaction process is still underway.

## Conclusion

In conclusion, we have developed a solution-phase template approach to synthesize $Cu_2S$ nanoribbons for the first time. $Bi_2S_3$ nanoribbons could act as both template and reactant in the reaction process. The as-prepared $Cu_2S$ nanoribbons were well characterized by XRD, FESEM, TEM and HRTEM, respectively. The intermediate products were also investigated, showing that different compositions of $Bi_2S_3$ and $Cu_2S$ also could be obtained through controlling the reaction time.

## Acknowledgements

This work is supported by the National Natural Science Foundation of China.

## References

1 J. T. Hu, T. W. Odom and C. M. Lieber, *Acc. Chem. Res.*, 1999, **32**, 435.
2 Y. N. Xia, P. D. Yang, Y. G. Sun, Y. Y. Wu, B. Mayers and B. Gates, *Adv. Mater.*, 2003, **15**, 353.
3 Z. W. Pan, Z. R. Dai and Z. L. Wang, *Science*, 2001, **291**, 1947.
4 Z. L. Wang, *Annu. Rev. Phys. Chem.*, 2004, **55**, 159.
5 Y. Ding, P. X. Gao and Z. L. Wang, *J. Am. Chem. Soc.*, 2004, **126**, 2066.
6 J. G. Yu, J. C. Yu, W. K. Ho, L. Wu and X. C. Wang, *J. Am. Chem. Soc.*, 2004, **126**, 3422.
7 X. B. Cao, Y. Xie, S. Y. Zhang and F. Q. Li, *Adv. Mater.*, 2004, **16**, 649.
8 B. Zhang, C. B. Cao, X. Xiang and H. S. Zhu, *Chem. Commun.*, 2004, 2452.
9 C. B. Murray, C. R. Kagan and M. G. Bawendi, *Science*, 1995, **270**, 1335.
10 A. P. Alivisatos, *Science*, 1996, **271**, 933.
11 V. Kilmov, P. H. Boilvar, H. Kurz, V. Karavanskii, V. Krasovskii and Y. Korkishko, *Appl. Phys. Lett.*, 1995, **67**, 653.
12 T. H. Larsen, M. B. Sigman, A. Ghezelbash, R. C. Doty and B. A. Korgel, *J. Am. Chem. Soc.*, 2003, **125**, 5638.
13 M. B. Sigman, A. Ghezelbash, T. Hanrath, A. E. Saunders, F. Lee and B. A. Korgel, *J. Am. Chem. Soc.*, 2003, **125**, 16050.
14 S. H. Wang and S. H. Yang, *Adv. Mater. Opt. Electron.*, 2000, **10**, 39.
15 J. Chen, S. Z. Deng, N. S. Xu, S. H. Wang, X. G. Wen, S. H. Yang, C. L. Yang, J. N. Wang and W. K. Ge, *Appl. Phys. Lett.*, 2002, **80**, 3620.
16 Z. P. Liu, S. Peng, Q. Xie, Z. K. Hu, Y. Yang, S. Y. Zhang and Y. T. Qian, *Adv. Mater.*, 2003, **15**, 936.